arXiv:1609.09139v1 [cond-mat.mtrl-sci] 28 Sep 2016

Modern Physics Letters B
© World Scientific Publishing Company

ALL-OPTICAL SPIN SWITCHING: A NEW FRONTIER IN FEMTOMAGNETISM A SHORT REVIEW AND A SIMPLE THEORY

G. P. Zhang*, T. Latta, and Z. Babyak

Department of Physics, Indiana State University, Terre Haute, IN 47809, USA
** gpzhang@indstate.edu*

Y. H. Bai

Office of Information Technology, Indiana State University, Terre Haute, IN 47809, USA

Thomas F. George

Office of the Chancellor and Center for Nanoscience
Departments of Chemistry & Biochemistry and Physics & Astronomy
University of Missouri-St. Louis, St. Louis, MO 63121, USA

Received (11 May 2016)

Using an ultrafast laser pulse to manipulate the spin degree of freedom has broad technological appeal. It allows one to control the spin dynamics on a femtosecond time scale. The discipline, commonly called femtomagnetism, started with the pioneering experiment by Beaurepaire and coworkers in 1996, who showed subpicosecond demagnetization occurs in magnetic Ni thin films. This finding has motivated extensive research worldwide. All-optical helicity-dependent spin switching (AOS) represents a new frontier in femtomagnetism, where a single ultrafast laser pulse can permanently switch spin without any assistance from a magnetic field. This review summarizes some of the crucial aspects of this new discipline: key experimental findings, leading mechanisms, controversial issues, and possible future directions. The emphasis is on our latest investigation. We first develop the all-optical spin switching rule that determines how the switchability depends on the light helicity. This rule allows one to understand microscopically how the spin is reversed and why the circularly polarized light appears more powerful than the linearly polarized light. Then we invoke our latest spin-orbit coupled harmonic oscillator model to simulate single spin reversal. We consider both cw excitation and pulsed laser excitation. The results are in a good agreement with the experimental result.[a] We then extend the code to include the exchange interaction among different spin sites. We show where the "inverse Faraday field" comes from and how the laser affects the spin reversal nonlinearly. Our hope is that this review will motivate new experimental and theoretical investigations and discussions.

Keywords: All-optical, spin switching, ultrafast

[a]A MatLab code is available upon request from the authors.

1. Introduction

In the course of magnetic recording, the types of magnetic materials and how one manipulates the spin moment are critical to the information technology industry. In normal magnetic storage media, the information is stored in magnetic domains of a few microns or less, with spin pointing in one direction called bit "1," and the other direction called "0." The external reading/writing head generates a small magnetic field, which switches those bits. Such a mechanism is used in normal hard drives. In a magneto-optical recording, one uses a laser beam to warm up the medium above the compensation point; when an external magnetic field is applied, the magnetic bit is switched over. However, there are some exceptions where a magnetic field is not used. In 1985, Shieh and Kryder[1] showed that in a GdTbCo film, the demagnetizing field[2] can effectively be used as a bias field for thermomagnetic writing without a magnetic field. This also works for GdTbCo, TbCo and TbFeCo thin films of several thousand angstroms thick. In their picture, the demagnetization field acts as a switching kernel. To understand how microscopically the switching process happens, the real time-dependent simulation of magnetic domain motion has been carried out.[2] This is a pre-femtomagnetism era, where the switching speed was not a major concern.

With the advent of ultrafast laser technology in the 80s and 90s, both electron and spin dynamics could be detected in the real time domain. Vaterlaus *et al.* [3] reported an interesting observation that the time scale for establishing thermal equilibrium between the lattice and spin system is 100±80 ps in ferromagnetic gadolinium. This was corroborated theoretically by Hübner and Bennemann.[4] A major breakthrough came when Beaurepaire and his coworkers[5] found that a 60-fs pulse could demagnetize the ferromagnetic nickel film within one picosecond (see Fig. 1). Such a short reduction was unexpected from the conventional spin wave theory, and motivated intensive research over two decades. The research of the first six years has been documented in our first review paper.[6] Kirilyuk and coworkers[7] summarized the research up to 2010. The reader may refer to these two review papers for those earlier studies. Kirilyuk and coworkers published another two review papers, one later[8] and one earlier,[9] but there are some overlaps among them. The development of femtomagnetism also appears in several monographs.[10,11,12,13,14]

Since our review mainly focuses on all-optical spin switching, we think that it is appropriate to review and give credit to some of those latest outstanding investigations that have greatly enriched our understanding of femtomagnetism and directly led to the discovery of all-optical spin switching.

After the discovery of femtomagnetism by Beaurepaire *et al.*,[5] almost immediately at least four different experimental techniques were used. Scholl *et al.*[15] employed spin-resolved two-photon photoemission to show that the Stoner excitation is responsible for the reduction of spin polarization over 1 ps, but unfortunately this result was never reproduced. Hohlfeld *et al.*[16] employed pump-probe second-harmonic generation (SHG) with 150-fs/800-nm laser pulses of various fluences

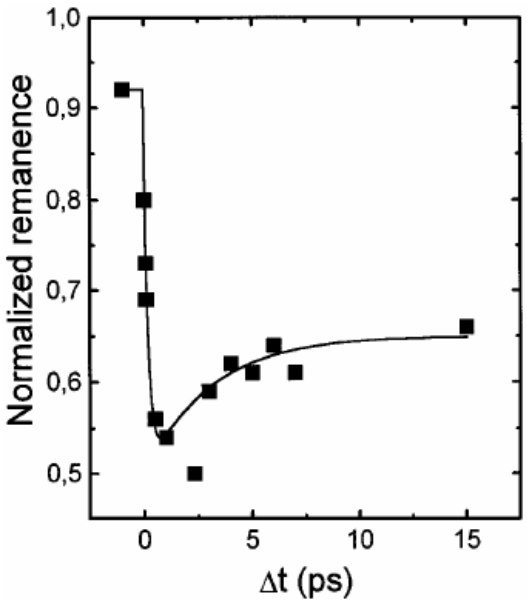

Fig. 1. Normalized remanence as a function of time delay between pump and probe pulses on a Ni(20 nm)/$MgFe_2$(100 nm) film. The pump fluence is 7 mJ/cm^2. Adopted from Beaurepaire *et al.*'s original work,[5] used with permission from the American Physical Society.

and demonstrated that the transient magnetization reaches its minimum at 50 fs. Aeschlimann *et al.*[17] employed time- and spin-resolved two photon photoemission to show that the lifetime of majority-spin electrons at 1 eV above the Fermi energy is twice as long as that of minority-spin electrons in fcc Co. La-O-Vorakiat *et al.*[18] developed a tabletop high-harmonic soft x-ray source to probe the demagnetization at the M edge of Fe and Ni. Koopmans *et al.*[19] questioned the validity of time-resolved magneto-optics to detect the spin change. Three subsequent studies by Guidoni *et al.*[20], Bigot *et al.*[21] and Vomir *et al.*[22] found that time-resolved magneto-optics can be reliably used, which was further clarified theoretically.[23] Regensburger *et al.*[24] investigated surface magnetism using time-resolved SHG. We proposed the first theory of ultrafast demagnetization[25] and showed that the cooperation between the laser field and spin-orbit coupling is crucial to understanding the ultrafast demagnetization. Ju *et al.*[26] extended research to exchange coupled systems and found a large modulation in the exchange bias field. Kise *et al.*[27] found the crossover from microscopic photoinduced demagnetization to macroscopic critical behavior, with a universal power law divergence of the relaxation time in half-metallic Sr_2FeMoO_6. Zhang *et al.*[28] showed that the magneto-crystalline anisotropy is modulated by nonthermal hot electron spins in another half-metallic CrO_2. More extensive studies were carried out by Müller *et al.*[29] They found that because the direct energy transfer by Elliot-Yafet scattering is blocked in a half-metal, the demagnetization

time is significantly slower.

Kimel *et al.*[30] discovered antiferromagnetic order quenching in $FeBO_3$. Rhie *et al.*[31] observed exchange splitting change in Ni. Gomez-Abal *et al.*[32] demonstrated that the switching in antiferromagnetic NiO is faster, which was confirmed experimentally by Duong *et al.*[33]. Satoh *et al.*[34] used circularly polarized pulses to drive spin oscillation in the fully compensated antiferromagnet NiO. Wang *et al.*[35] demonstrated a similar quenching of ferromagnetism in InMnAs and enhancement of ferromagnetism in GaMnAs.[36] Stamm *et al.*[37] claimed that the quenching of spin angular momentum and its transfer to the lattice, with a time constant of 120±70 fs, is determined unambiguously with x-ray magnetic circular dichroism. Such an unusual fast time scale is surprising. Koopmans *et al.*[38] showed that a model based on electron-phonon-mediated spin-flip scattering explains both timescales on equal footing, but Carva *et al.*[39] showed that the Elliott-Yafet electron-phonon effect is extremely small. Theoretically, Mueller *et al.*[40] suggested a dynamical Elliott-Yafet mechanism to dynamically modify the Stoner exchange splitting to get the same amount of the spin moment reduction as seen in the experiment, and they suggested that in general Elliott-Yafet microscopic picture of demagnetization dynamics is viable. Very recently, Bonetti *et al.*[41] demonstrated that only the amorphous GdFeB sample shows ultrafast demagnetization caused by the spin-lattice depolarization of the THz-induced ultrafast spin current. Quantitative modeling shows that such spin-lattice scattering events occur on similar time scales as conventional spin conserving electronic scattering (about 30 fs). A recent study of the phonon angular momentum transfer found a very small effect, with the rate of change on the order of $0.06\ \hbar/100$ fs.[42] To diminish the fcc Ni spin moment takes 1 ps. Thus, the phonon is unlikely the main course of demagnetization over a few hundred femtoseconds, as already shown by Lefkidis *et al.*,[43] but there is currently no agreement on this.

Andrade *et al.*[44] studied the response of the magnetization vector of superparamagnetic nanoparticles and showed that the magnetization precession is damped more quickly in the superparamagnetic particles than in cobalt films. Pickel *et al.*[45] investigated how the spin-orbit hybridization bands are changed in fcc Co and demonstrated that these spin hot spots enhance spin-flip scattering. We showed that the spin and orbital momentum excitation proceed on different time scales.[46] Schmidt *et al.*[47] demonstrated that magnon emission by hot electrons occurs on the femtosecond time scale. Battiato *et al.*[48] proposed superdiffusive spin transport as a mechanism of ultrafast demagnetization. Rudolf *et al.*[49] showed that indeed ultrafast magnetization enhancement in metallic multilayers is driven by a superdiffusive spin current. Eschenlohr *et al.*[50] moved one step further and declared the ultrafast spin transport as key to femtosecond demagnetization. Vodungbo *et al.*[51] thought that Eschenlohr *et al.*'s study does not unambiguously prove that part of the magnetization is transferred to the metallic cap layer via superdiffusive spin transport. Instead, they claimed that their data undoubtedly prove that the ultrafast demagnetization process can be triggered without any direct interaction between the photons of the optical pump pulse and the magnetic layer. They also

emphasized that even though their results appear in agreement with the superdiffusion prediction, this is not evidence or proof of superdiffusion. A true verification of spin superdiffusion requires a measurement of the spin that is diffused out of the magnetic sample, which was not done in their experiment.[51] Turgut *et al.*[52] used multilayers of Fe and Ni with different metals and insulators as the spacer material to conclusively show that spin currents can have a significant contribution to optically-induced magnetization dynamics, in addition to spin-flip scattering processes. Schellekens *et al.*[53] found that the temporal evolution of the magnetization for front-side and back-side pumping in Ni thin films is identical, so that no influence of transport is detected. Whether superdiffusion is important is hotly debated for the moment.

Besides those common transition metals, rare earth metals were also investigated. Lisowski *et al.*[54] used time-resolved photoemission and magneto-optics to investigate the spin dynamics on a Gd(0001) surface, and proposed a mechanism of electron-magnon interaction to facilitate electron-spin-flip scattering among spin-mixed surface and bulk states. Melnikov *et al.*[55] looked at magnetic linear dichroism at a core-level photoemission and showed that equilibration between the lattice and spin subsystems takes about 80 ps in Gd. Radu *et al.*[56] explored the effect of Ho, Dy, Tb, and Gd impurities on the femtosecond laser-induced magnetization dynamics of thin Permalloy films using the time-resolved magneto-optical Kerr effect, and found a gradual change of the characteristic demagnetization time constant from 60 to 150 fs. In Gd and Tb, Wietstruk *et al.*[57] observed a two-step demagnetization with an ultrafast demagnetization time of 750 fs, identical for both systems, and slower times which differ with 40 ps for Gd and 8 ps for Tb. Carley *et al.*[58] employed the high-order harmonic generation technique[18] to investigate the temporal evolution of the exchange-split bands and found an ultrafast drop of the exchange splitting. There is a difference in the ultrafast dynamics between itinerant and localized magnetic moments in gadolinium metal.[59]

Kim *et al.*[60] extended the study to ultrafast magnetoacoustics and showed that the propagating strain associated with the acoustic pulses modifies the magnetic anisotropy and induces a precession of the magnetization. Theoretically, the time-dependent density functional theory was implemented to investigate the spin moment change.[61] Recently, we developed a new technique to couple the time-dependent Liouville equation with the density functional theory, where we found that the functional is extremely important to yield the same amount of the spin reduction.[62]

To start with, we would like to add a word of caution on the name conventions used in the all-optical spin switching. All-optical spin switching, or AOS, may appear in the literature as all-optical helicity-dependent spin switching or AO-HDS or AOS. All-optical helicity-independent spin switching, AO-HIDS, is called "thermal switching" in the literature. Using the word "thermal" is confusing, since a true thermal process should only pertain to the temperature gradient across a sample from a slow heating source. Many research papers do not distinguish the thermal

equilibrium among the electrons or between the electron and phonon subsystems. In some studies, the linearly polarized laser pulse is called a heating pulse. This is also inappropriate since the linearly polarized light also changes the orbital angular momentum $\Delta l = \pm 1$. The helicity-independent demagnetization is called thermal demagnetization (TD). Conceptually, this is also problematic, since there is a clear distinction between a true thermal source driven and laser-driven demagnetization, in particular, on the time scale of a few hundred femtosecond to 10 ps. In this paper, we prefer to use AO-HDS and AO-HIDS. Whenever possible, we will state clearly what the thermal effect indeed refers to. Another confusion is that many researchers also use the time-dependent temperature. Temperature is a statistical concept, averaged over a period of time. What is really meant here is the nonequilibrium population distribution is created in the time domain.

The rest of the paper is arranged as follows. In Section II, we review the essential experimental findings. Since there are many groups contributing to the same topics, we group them into five major topics: (1) Dependence on the sample temperature and compensation temperature; (2) Dependence on laser parameters; (3) Composition dependence; (4) Beyond GdFeCo; and (5) Proposed mechanisms. Since some of those topics slightly overlap, we prefer to repeat the same information in each of those relevant subsections. Section III is devoted to the phenomenological theory, which is the most popular theory at this time. In Section IV, we review our microscopic theory of spin reversal, starting from the optical spin switching rule, the single model under cw excitation, spin reversal theory under pulse laser excitation, inclusion of exchange coupling, demonstration of the inverse Faraday effect, and finally the effect of the laser field amplitude on spin reversal. Section V presents some new techniques and possible new directions. Finally, we conclude this paper in Section VI.

2. Experimental findings

Different from the magnetic field-driven spin reversal, AOS relies on a laser field to switch spin from one direction to another. Figure 2 shows that left-circularly polarized light can switch a spin from down to up, while right-circularly polarized light can switch a spin from up to down. This is considered remarkable since the laser field (E-field) does not directly interact with the spin degree of freedom.

In 2007, Stanciu and coworkers[63] reported that a single 40-fs laser pulse, free of any magnetic field, could switch the spin in $Gd_{22}Fe_{74.6}Co_{3.4}$ from one direction to another (Fig. 3). If left-circularly polarized light (LC) switches the spin from down to up, then right-circularly polarized light (RC) switches the spin from up to down. Linearly polarized light (LP) induces small domains with spin randomly oriented up or down. This is the beginning of AO-HDS. Different from regular ferromagnetic thin films, GdFeCo is very complex. Structurally, metallic $Gd_{22}Fe_{74.6}Co_{3.4}$ is amorphous, posing a big challenge for a direct simulation which requires the structural information. Optically, the material is highly absorptive. Magnetically,

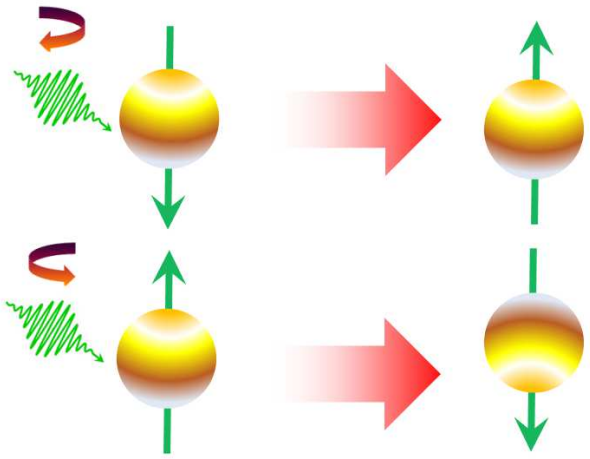

Fig. 2. Left-circularly polarized light can switch a spin from down to up, while right-circularly polarized light can switch a spin from up to down. A magnetic field is not needed.

two magnetic sublattices are coupled ferromagnetically, i. e., the coupling between Gd ions and that between Fe ions are ferromagnetic. But the coupling between Gd and Fe is ferrimagnetic, with the exchange interaction on the order of meV.[64,65] $Gd_{22}Fe_{74.6}Co_{3.4}$ has a saturation magnetization of 1000 G at room temperature and Curie temperature of 500 K.

AOS depends on the sample's temperature, compensation temperature, composition, and laser parameters. To understand the microscopic mechanism of how AOS works, one has to disentangle the convoluted effects both intrinsically and extrinsically. In the following, we make a moderate attempt to present crucial experimental facts, even when they sometimes are contradictory among themselves.

2.1. *Dependence on sample and compensation temperature*

One unique feature of ferrimagnets is that the system has two magnetic sublattices, A and B. Here A refers to Gd and B refers to Fe/Co. The spin moments on A and B are different and in the opposite direction. We define the compensation temperature when the spin moments from sublattices are equal in magnitude but point in the opposite direction. Thus they cancel each other out, and the net magnetization of the entire sample drops to zero.

Vahaplar *et al.*[66] found that the optimal conditions for the all-optical reversal are achieved just below the ferrimagnetic compensation temperature. The sample

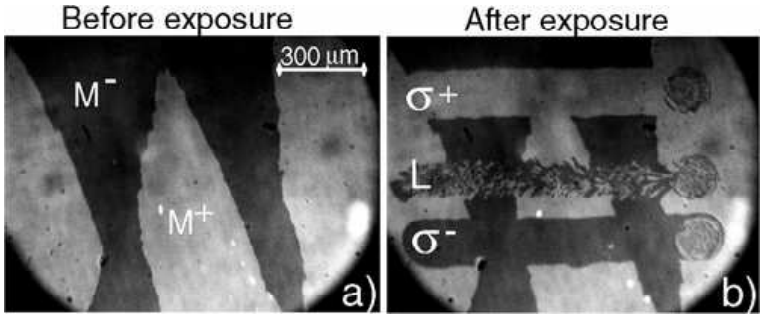

Fig. 3. All-optical spin switching in $Gd_{22}Fe_{74.6}Co_{3.4}$ demonstrated by Stanciu *et al.*[63] (a) Magneto-optical image of the initial magnetic state of the sample before laser exposure. White and black areas correspond to up (M^+) and down (M^-) magnetic domains, respectively. (b) Magnetic domains after sweeping at low speed μm/s linear (L), right-handed (σ^+), and left-handed (σ^-) circularly polarized beams across the surface of the sample, with a laser fluence of about 11.4mJ/cm^2. The circularly polarized light switches the magnetization, but the linearly polarized light breaks up the domains. Used with permission from the American Physical Society.

temperature also influences how large the laser fluence should be in order to switch spins.[66] The larger the deviation of the sample temperature from the compensation temperature, the higher the laser fluence required for the switching.[66] Vahaplar *et al.* suggested that choosing temperature in the vicinity of the compensation temperature is very important for the spin reversal. Hohlfeld *et al.*[67] showed that too high a temperature is detrimental to AOS. In an earlier study,[68] Vahaplar *et al.* found that the spin reversal time in $Gd_{24}Fe_{66.5}Co_{9.5}$ is on the order of 90 ps, and does not change much among GdFeCo alloys if the sample temperature is below the compensation temperature. But once the temperature is above the compensation temperature, the time increases sharply.

However, the above finding is not generic across all AOS materials. In 2013 Hassdenteufel *et al.*[69] found that AOS in Tb_xFe_{100-x} occurs below and above the magnetic compensation point, and they even found that AOS takes place in samples without a compensation temperature.

2.2. *Dependence on laser parameters*

The dependence of the laser fluence on the AOS was first explored. Stanciu *et al.*[63] showed that at a laser fluence of 2.9 mJ/cm^2, only one type of helicity, LC or RC, can reverse the spin. When they increased the fluence to 5.7 mJ/cm^2, regardless of the laser helicity, multiple domains were formed after the laser exposure. Vahaplar *et al.*[68] found that AOS in $Gd_{22}Fe_{68.2}Co_{9.8}$ only occurs in a narrow fluence range, and the switchability forms a "Λ" shape (see Fig. 4).[b] In $Gd_{24}Fe_{66.5}Co_{9.5}$

[b]We note in passing that their fluence has a unit of J/m^2, but in their latter paper,[66] they changed it back to mJ/cm^2, so it is difficult to know at present which unit they referred to.

and $Gd_{26}Fe_{64.7}Co_{9.3}$ the reversal window gets wider as the laser pulse duration increases.[66] Chen *et al.*[70] directly measured the hysteresis loop in $Gd_{23.5}Fe_{73.2}Co_{3.3}$ as a function of the external magnetic field with and without the pump pulse. Interestingly, they found that the hysteresis becomes anomalous, consistent with Stanciu *et al.*, [71] and is no longer a square shape. Instead, the domain breaks into different parts, some of which become irreversible. This is reflected on the hysteresis loop. Stanciu *et al.*[71] also performed a laser fluence-dependent study of the hysteresis and found that when the pump fluence is higher, the spin first relaxes in the opposite direction; then once the system cools down, the spin reverses back to the initial configuration.

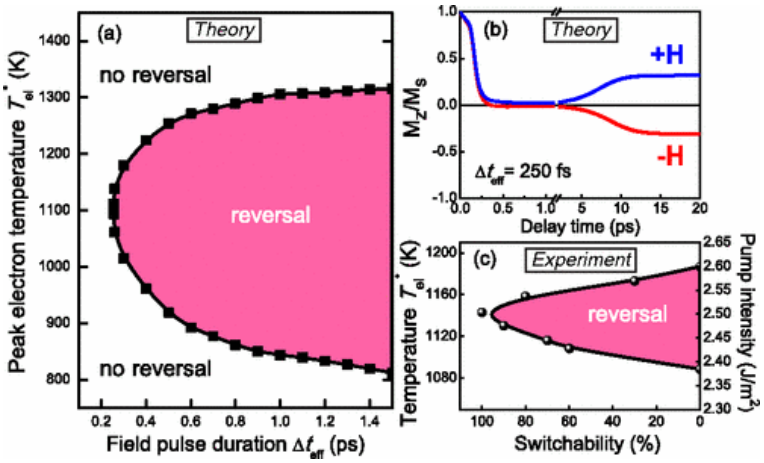

Fig. 4. Spin reversal only occurs in a narrow region. (a) Theoretical results from the phenomenological simulation. (b) Magnetic field-driven switching. (c) Experimental results. Note that the shape is skinny, different from the theory.[68] Used with permission from the American Physical Society.

A similar fluence dependence in $Gd_{26}Fe_{65}Co_9$ was carried out by Khorsand *et al.*[72] who showed that the switching probability increases with the fluence, but differently for left-circularly polarized light, right-circularly polarized light and linear polarized light. They explained the difference by different optical absorption efficiencies among different helicities. The effective switching threshold is independent of the wavelength, at 2.6 ± 0.2 mJ/cm^2, which is lower than $Gd_{26}Fe_{64.7}Co_{9.3}$.[66]

A more systematic investigation of the effect of the laser parameters, including, the laser pulse duration, wavelength, chirp and bandwidth, was performed by Steil *et al.*[73] They showed that AOS in $Gd_{26}Fe_{64.7}Co_{9.3}$ can be achieved with a picosecond laser as well, and the microscopic process seems only to depend on the number of photons.

Alebrand *et al.*[74] provided a much needed insight. They employed different

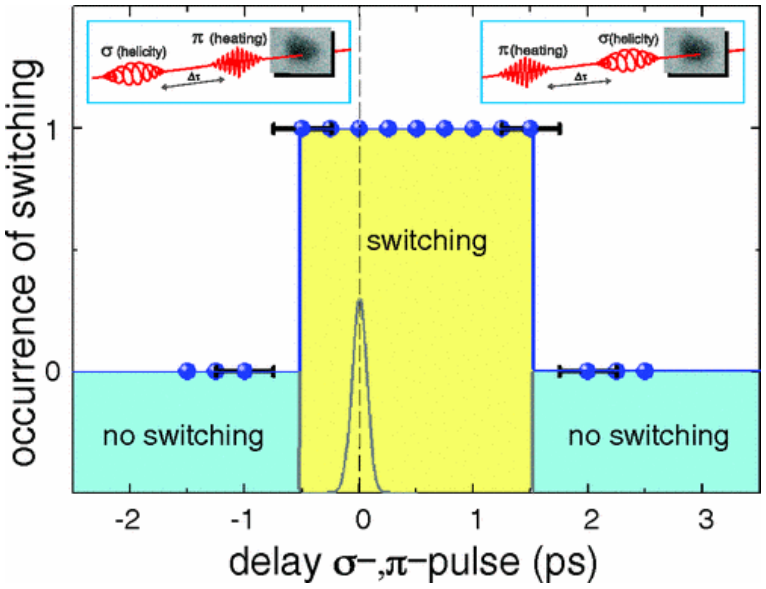

Fig. 5. Occurrence of switching as a function of time delay between σ and π pulses. Only a limited switching window is observed.[74] Used with permission from the American Physical Society.

combinations of two laser pulses, one linearly polarized light (π) and the other circularly polarized light (σ) (see Fig. 5). Their goal was to distinguish the effects of heating and helicity of the laser pulse. Their idea is that the σ pulse carries the helicity information while the π pulse provides heating. Using different combinations, one may be able to differentiate the roles of the laser pulse from others. Before we proceed, we note that both σ and π carry the helicity information and heating. Their sample was $Gd_{24}Fe_{66.5}Co_{9.5}$, with out-of-plane magnetization, compensation temperature of 280 K and Curie temperature of 500 K. The central wavelength of their laser is 780 nm, with pulse duration changeable from 90 fs to 2 ps. They first used a single σ pulse and lowered its fluence until no switching is observed, and then they added a π pulse. They found that the switching becomes possible again as far as these two pulses overlap spatially and temporally. If they increased the π pulse fluence further, a helicity-independent demagnetization was observed.The total threshold fluence for the $\sigma - \pi$ combination is always higher than a single σ pulse minimum threshold fluence. This indicated that the switching does not only depend on the number of photons, different from their original finding,[73] but also on the helicity. The circularly polarized light appeared more powerful. They also decreased the σ pulse fluence and found that there exists a smaller threshold for the σ pulse once the π pulse is on. However, once the fluence for the σ pulse is below the above lower threshold, increasing the π fluence can not lead to switching. Instead, a pure demagnetization (helicity independent) occurs.

Alebrand *et al.*[74] also investigated how the minimum threshold fluence of the circularly polarized light depends on the laser repetition rate, and they found that as the repetition rate increases from 0 Hz to 500 kHz, the required minimum fluence drops from 6 to 1.5 mJ/cm^2. It is unclear whether this finding is related to a recent study by El Hadri *et al.*[75] who employed the Hall cross to characterize the switching,[76] and found that in GdFeCo the switching is "single pulse" instead of "cumulative."

2.3. *Composition dependence*

The investigation of the composition effect on AOS is much more extensive than any other studies because AOS does not happen in any composition. This is easy to see this from their element spin moments. Gd has nearly zero orbital angular momentum since its 4f orbital is half-filled, but the spin moment is big, and in pure Gd metal it is 7.63 μ_B.[77,78] By contrast, iron has a spin moment of 2.2 μ_B. The small composition of Co is to control the perpendicular anisotropy.[79]

Vahaplar *et al.*[66] employed five different compositions: $Gd_{20}Fe_{70}Co_{10}$, $Gd_{22}Fe_{68.2}Co_{9.8}$, $Gd_{24}Fe_{66.5}Co_{9.5}$, $Gd_{26}Fe_{64.7}Co_{9.3}$, and $Gd_{28}Fe_{63}Co_9$. With the same laser fluence, duration and polarization, they showed that different compositions of Gd ions have a significant effect on AOS. At 3.14 mJ/cm^2, only $Gd_{26}Fe_{64.7}Co_{9.3}$ shows helicity-dependent switching, while $Gd_{22}Fe_{68.2}Co_{9.8}$ and $Gd_{24}Fe_{66.5}Co_{9.5}$ show helicity-independent switching. But by lowering the pump fluence, $Gd_{22}Fe_{68.2}Co_{9.8}$ and $Gd_{24}Fe_{66.5}Co_{9.5}$ also show helicity-dependent switching. However, $Gd_{20}Fe_{70}Co_{10}$ is very different from the rest of the compositions. A single laser of any polarization only leads to a multidomain state. This clearly demonstrates the decisive role of the composition in AOS. Future research should focus on much more on this interesting development.

The composition effect is also observed in Tb_xCo_{1-x} alloys. Alebrand *et al.*[80] showed that the optical magnetization switching is observed only for $x = 26\%, 28\%$ and 30%. It is in this composition region where the compensation temperature is higher than the room temperature but lower than the Curie temperature. From this study, it is clear that composition plays a decisive role here too, but it is unclear whether the compensation temperature is a result of composition or the cause of AOS. In a latter study,[81] they reported that in $Tb_{32}Co_{68}$ a transient magnetization reversal occurs on both sublattices on a subpicosecond time scale, but AOS was not observed in this compound. This may indicate that a transient reversal is not a necessary precursor to spin reversal, as it is in GdFeCo[82] and TbFe[83] where a transient ferromagnetic-like state is identified before spin reversal, but their technique is not really element-specific, and their entire observation relied on the wavelength dependence. In $Tb_{26}Co_{74}$ where AOS was observed, a transient reversal was observed again, but only at a probe wavelength of 800 nm and at a high laser fluence of 2.4 mJ/cm^2. In summary, since their technique is not really element-specific, it is difficult to determine whether the actual spin reversal occurred (or

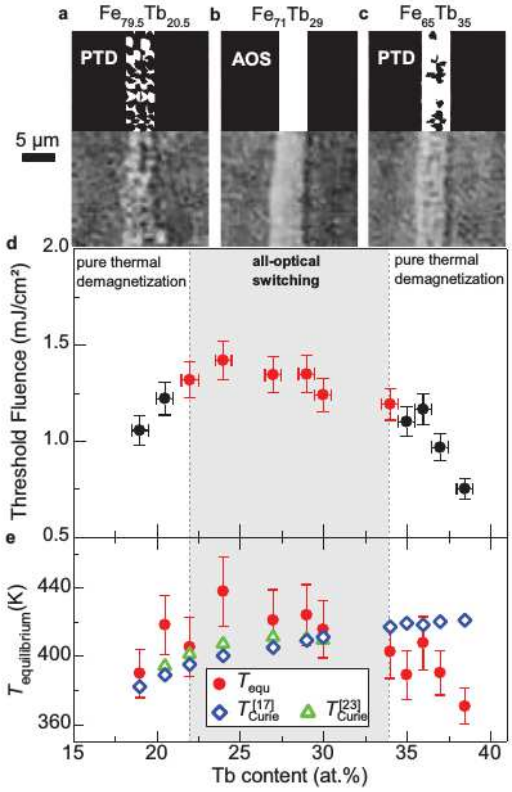

Fig. 6. In Tb_xFe_{100-x}, AOS occurs only between $x = 22\%$ and $x = 34\%$.[69] Used with permission from Advanced Materials.

not) at which site Co or Tb.

In 2013, Hassdenteufel *et al.*[69] systematically investigated the role of the composition on the AOS in Tb_xFe_{100-x} and found that AOS occurs only between $x = 22\%$ and $x = 34\%$. Outside this composition range, only helicity-independent demagnetization is observed (see Fig. 6).

Mangin *et al.*[84] summarized the trend for AOS in different compounds. In GdFeCo, the Gd composition must be between 25% and 30%; in TbCo, the Tb composition between 22% and 26%; in DyCo with Dy composition between 26% and 29%; in HoFeCo with Ho composition between 23% and 26%; in TbCo multilayers, 17%-32%; and in HoCo, the Ho composition must be between 22% and 31%. The understanding of these distinctive composition dependencies is lacking.

2.4. *Beyond GdFeCo*

Most AOS materials are GdFeCo and its variants with different compositions. As discussed above, Alebrand *et al.*[74] discovered spin switching in TbCo alloys, while Hassdenteufel *et al.*[69] showed TbFe works as well. In 2014, Mangin *et al.*[84] discovered that the rare-earth-free Co-Ir-based synthetic ferrimagnetic heterostructures are also AOS materials. AOS is found in Co(0.5nm)/Tb(0.4nm) multilayers, but not Co(0.8nm)/Tb(0.4nm). Note that AOS only favors ultrathin Co, a peculiar feature that is not yet understood. Lambert and coworkers[85] showed that AOS occurs in ultrathin ferromagnetic CoPt films. The number of repeats is between 2 and 3; if higher than this, only helicity-independent demagnetization is found. The thickness of the Co layer must be below 1.0 nm; and the laser power threshold is below 500 nW. By increasing the Ni concentration, one gets thermal demagnetization, not AOS. These stringent conditions are interesting and useful for future research. There is some similarity between different AOS materials. Some simulations on ferromagnets have appeared,[86,87] but a complete picture is missing. In particular, there has been very few independent studies from other groups.

2.5. *Proposed mechanisms*

So far, there are several mechanisms proposed. According to Kirilyuk *et al.*[7] the interactions between the laser and magnetic systems fall into three categories: (a) thermal effects, (b) nonthermal photomagnetic effects, and (c) nonthermal optomagnetic effects. Optomagnetism refers to a magnetic process where the system does not directly absorb the light energy, but may interact with other elementary excitations such as phonons or magnons. Photomagnetism refers to a magnetic process where the system absorbs energy from the light field.

Stanciu *et al.*[63] suggested stimulated Raman scattering for AOS that involves angular momentum transfer from the lattice to the spins. Their suggestion was based on a simple estimate that switching due to direct transfer of angular momentum via absorption is unlikely. However, Hohlfeld *et al.*[67] looked at the temperature dependence of AOS on the same metallic sample as Stanciu *et al.*[63] Hohlfeld *et al.* found that at 2.5 mJ/cm^2, which is below the laser fluence threshold of about 3 mJ/cm^2, the switching is not possible between 250 and 300 K, but as the temperature is lowered, switching occurs. They concluded that increasing the temperature reduced the efficiency of the AOS, which invalidated the original ideas based on stimulated Raman-like scattering.[63] This result is consistent with the study with different substrates.[88] Hassdenteufel *et al.* showed that for $Tb_{30}Fe_{70}$, AOS occurs on the SiO_2/Si substrate but not on the microscope glass slide.[88] It seems that heating accumulation with a higher temperature is detrimental to AOS.

Vahaplar *et al.*[68] suggested the inverse Faraday effect as the driving field to AOS. In 2012, Ostler and coworkers[79] found that when the laser fluence is above a certain threshold value at which Vahaplar *et al.*[68] found helicity-dependent switching, the switching is helicity-independent. Ostler *et al.* claimed that their new ob-

servation negates their own explanation based on the inverse-Faraday effect. They called this new AOS a thermal effect (i.e., helicity-independent switching). This result leads to some confusion and needs an explanation, since apparently phenomenological models reach their limit of prediction. To clarify the situation, we notice that, according to Ostler *et al.*, to go from helicity-dependent to helicity-independent spin switching, one only needs to increase the laser fluence by as little as 0.05 mJ/cm^2. This is rather surprising. We estimate that for a 0.05 mJ/cm^2 change in fluence, the photon number increases by 0.05 photon.[89] It is unclear as to how reliable their characterization is. This problem remains unsolved.

Steil *et al.* showed that while the concept of an induced effective magnetic field H_{eff} agreed with their experimental results,[73] the field could not be explained in terms of an inverse Faraday effect nor spin-flip stimulated Raman scattering. They also wondered where the helicity information is stored after the duration of the laser pulse. A few years earlier, Stanciu *et al.*[63] already argued that the actual magnetization reversal must take place on a subpicosecond time scale, since the interaction between the laser field and the sample lasts only 40 fs (pulse duration). This is the only way for the helicity information to survive on a long time scale. Otherwise, why doesn't the lattice mess up the angular momentum?

Khorsand *et al.*[72] proposed magnetic circularly dichroism (MCD) as the underlying mechanism for AOS. They claimed that they could quantitatively explain AOS using MCD. What they did is to compare the inverse Faraday effective magnetic field with magnetic circularly dichroism or magnetic circular birefringence, and to see which one has a larger effect. There is no actual time-dependent simulation to prove that MCD is responsible for AOS. Therefore, it may be too early to claim quantitative proof as it intrinsically excludes other possible mechanisms. It may be more appropriate to consider all the possible scenarios before a definitive statement can be made. For instance, they initially insisted that AOS is an optomagnetic process,[66] but now they favor the photomagnetic process, where the AOS depends on the amount of energy absorbed from the laser.[72]

In searching for the essence of AOS, Schubert *et al.*[90] proposed that the low remanent magnetization is a key prerequisite for AOS. They chose $Tb_{36}Fe_{64}$ and $Tb_{19}Fe_{81}$, none of which shows AOS. But when they exchange coupled them to form a heterostructure with zero spin moment, then AOS occurs in the combination. This demonstrates the importance of remanence on AOS. This low-remanence criterion was further reinforced by Hassdenteufel *et al.*[91] They found that a low remanent sample magnetization is crucial for all-optical magnetic switching in ferrimagnets and ferrimagnet heterostructures. For nearly all the AOS materials, the remanence is below 220 emu/cc. The small remanence criterion, if verified by other groups, is extremely interesting. In 2013, Barker *et al.*[92] suggested that a two-magnon bound state causes ultrafast thermally-induced magnetization switching.

3. Phenomenological theory

Since the discovery of AOS by Stanciu *et al.*,[63] several theoretical approaches have appeared. However, the majority are phenomenological and do not have actual calculations. Gridnev[93] developed a theory for a transparent magnetic dielectric, where the key interaction is impulsive stimulated Raman scattering. The time dependence of the effective field is approximated by a δ-function. However, in the real experiment,[63] GdFeCo is metallic and not transparent, so that a direct application of the theory to those materials is difficult. Along the same line, Popova *et al.*[94] adopted a hydrogenlike system. They employed the same technique used by Lefkidis *et al.*[95] and were able to factor out the induced magnetization. The insight they revealed is that in contrast to the previous belief in the inverse Faraday effect, where the effective magnetic field is proportional to $\mathbf{E}(t)^* \times \mathbf{E}(t)$, the actual effective magnetic field is much more complicated. Only in the limit of a very long pulse or cw wave is the above relation restored, which is already clear from the original work by Pershan *et al.*[96] The same conclusion is found under the Drude-Lorentz approximation.[97] Unfortunately, $\mathbf{E}(t)^* \times \mathbf{E}(t)$ is still in use up to now. In 2013, Gridnev[98] proposed an interesting approach where the itinerant electrons are heated by the laser. The spin polarization is changed through the rate equation but augmented by a spin generating function G. G is proportional to the laser intensity multiplied by a conductivity tensor and energy conservation δ-function. This approach is reasonable if under cw excitation, but when using a pulsed laser, this is not appropriate, since G changes as the laser field. Therefore, in the real calculation, the author replaced G by a special initial value of the spin, which makes the theory highly empirical.

Ostler *et al.*[99] employed fcc cells under periodic boundary conditions, where the transition metal (TM) and rare-earth (RE) ions are randomly distributed. Such a procedure does not take into the distance between ions. The entire system is described by the following Hamiltonian:

$$H = -\frac{1}{2}\sum_{ij} J_{ij}\mathbf{S}_i \cdot \mathbf{S}_j - \sum_i D_i(\mathbf{S}_i \cdot \mathbf{n}_i)^2 - \sum_i \mu_i \mathbf{B} \cdot \mathbf{S}_i. \quad (1)$$

Here, J_{ij} is the exchange integral between spins at site i and j, $\mathbf{S}_i$ is the normalized vector $|\mathbf{S}_i| = 1$, D_i is the uniaxial anisotropy vector, μ_i is the magnetic moment of the site i, and $\mathbf{B}$ is the vector describing the applied field. Their exchange integrals are $J_{\mathrm{TM-TM}} = 0.0281$ eV between TMs, $J_{\mathrm{RE-RE}} = 0.00787$ eV between REs, and $J_{\mathrm{TM-RE}} = -0.0068$ eV between TM and RE. These values are somewhat changed in their later studies.[79] It is clear that such a Hamiltonian can not describe the AOS, since there is no laser field. To overcome this difficulty, Vahaplar *et al.*[66] introduced an optomagnetic field $\mathbf{H}_{\mathrm{OM}}$ by considering the fact that a circularly polarized subpicosecond laser pulse can act on spins as an effective light-induced magnetic field. Specifically they used a phenomenological expression from the inverse Faraday effect derived for a transparent medium in thermodynamic equilibrium under

cw excitation,

$$\mathbf{H}_{\mathrm{OM}}(t,r) = \epsilon_0 \beta [\mathbf{E}(t,r) \times \mathbf{E}^*(t,r)], \tag{2}$$

where ϵ_0 is the permittivity in vacuum, β is the magneto-optical susceptibility, and $|\mathbf{E}(t,r)|$ is the envelope of the laser E-field. Some comments are necessary. First, Eq. (2) is conceptually very simple, but the cross product of two electric fields $\mathbf{E}$ carries different spatial indices,[100] which are coupled with β; otherwise, the cross product between two identical vectors is zero. For this reason, they had to introduce another coefficient σ, which is ± 1 for left- and right-circularly polarized light and is 0 for linearly polarized light. In other words, linearly polarized light has a zero $\mathbf{H}_{\mathrm{OM}}$, at variance with the experimental findings.[63,79] There is some inconsistency here. Second, the original expression is obtained under cw excitation, but here a pulse laser is used. If one uses $\mathbf{H}_{\mathrm{OM}}$, then the entire effective field would have the same duration as the laser field, which is 40 fs in their case. To overcome this issue, they split their $\mathbf{H}_{\mathrm{OM}}$ into two half-pulses. The first half follows the laser field, and the second half does not. Under the above approximation, they solved the Landau-Lifshitz-Gilbert equation to compute the spin reversal.

An extension to the above study was made by Wienholdt *et al.*,[101] who separated the spins according to their orbital characters, such as d and f. The entire simulation is similar to Ostler *et al.*[79] The laser effect is simulated by a temperature increase, which is normal for this kind of simulation. They also found transient ferromagnetic ordering.

Another approach is based on the multisublattice magnets. Mentink *et al.*[102] coupled the multisublattice to a heat bath with a time-dependent temperature. The laser field is ignored, and instead is replaced by a time-dependent temperature. Since temperature is a statistical concept, introducing a time-dependent temperature is questionable, but a phenomenological theory was useful in the beginning of AOS investigation.

Assuming an inverse Faraday effect, Petrila *et al.*[103] investigated the dependence of AOS on the laser parameters. A similar approach was employed by Cornelissen *et al.*,[86] who developed another model simulation to address switching in the Co/Pt system. This was an interesting approach as it does not involve some complicated calculation.

Chimata *et al.*[104] carried out an investigation on a supercell with 200 Gd and Fe atoms with amorphous structures at the first-principles level, but only at the static structure and magnetic properties level. This represents an important improvement over the previous studies. However, for spin switching, they still used the Landau-Lifshitz Gilbert equation, so there is no laser pulse in the simulation; instead they used an effective magnetic field and electron temperature. As a result, only the thermal switching was investigated. They found the thermal switching was observed for all the cases, regardless of whether the initial temperature was above or below a compensation temperature.

Baral and Schneider[105] adopted a model that couples the local spins with itin-

erant spins antiferromagnetically. They showed that with a sufficiently strong laser, a transient ferromagnetic-like state can always appear, but this state only results in true spin switching when the model parameters yield the compensation point.

4. A simple all-optical spin switching theory

To this end, it is very difficult to develop a comprehensive theory for all-optical spin switching. AOS materials are very diverse and very complex; some of them are amorphous. From the above discussion, we have seen nearly all theoretical investigations are phenomenological and mostly build upon an effective magnetic field. But the interest in AOS is a magnetic field-free spin reversal. Encouraged by the recent finding of AOS in ferromagnet CoPt,[85] we find a simple way to understand AOS. Most of the materials here are unpublished and first presented in this review. The initial finding is very attractive. For this reason, we provide a MatLab code for our theory, so the reader, in particular, the experimentalist, can directly adopt it to explain their experimental results, though our MatLab code[c] does not include the exchange interaction for the moment.

4.1. *Optical spin switching rule among spin-orbit coupled states*

All-optical spin switching is an optical process, so it must obey the dipole selection rule.[106] But common selection rules are often restricted to pure spin states, so the spin is unchanged. We choose two sets of spin-orbit coupled states, where the total angular momentum quantum number j and the magnetic one m_j are good quantum numbers. One may consider these states as a basis of the eigenstates for a solid, and they take a significant weight on the true wavefunctions. Materials of different kinds may have different weights on those states and lead to either demagnetization, magnetization or spin reversal, or any combination of them. To develop an analytic expression for the spin switching is difficult if we directly adopt the eigenstates of solids, partly because the true physics of AOS is mostly hidden in the lengthy summation over band states.

In the following, we consider two spin-orbit coupled states, ψ_a and ψ_b,[106]

$$\psi_a = \sqrt{\tfrac{l+m+1}{2l+1}}Y_{lm}|\alpha\rangle + \sqrt{\tfrac{l-m}{2l+1}}Y_{lm+1}|\beta\rangle, \quad \text{for } j = l+1/2, m_j = m+1/2, \tag{3}$$

$$\psi_b = -\sqrt{\tfrac{l-m}{2l+1}}Y_{lm}|\alpha\rangle + \sqrt{\tfrac{l+m+1}{2l+1}}Y_{lm+1}|\beta\rangle, \quad \text{for } j = l-1/2, m_j = m+1/2, \tag{4}$$

where $|\alpha\rangle$ and $|\beta\rangle$ refer to the spin-up and spin-down eigenstates, and Y_{lm} is spherical harmonic with angular and magnetic angular quantum number l and m, respectively. l and m in Eqs. (3) and (4) may differ from each other. We should point out that the transition between ψ_a states or between ψ_b states changes the total angular

[c]This code will be published in our book entitled *Introduction to Ultrafast Phenomena: From Femtosecond Spin Dynamics to Attosecond High Harmonic generation* by G. P. Zhang, W. Hübner, G. Lefkidis, A. Rubio and T. F. George (CRC, Boca Raton, FL, 2018).

Table 1. Spin switchability η of all-optical spin reversal among spin-orbit coupled states. For all $\Delta j = -1$ cases, j must be no less than 3/2. LP refers to linearly polarized light, LC left-circularly polarized light, and RC right-circularly polarized light.

	LP ($\Delta m_j = 0$)	LC ($\Delta m_j = +1$)	RC($\Delta m_j = -1$)
$\eta^{a\to a'}$ $\Delta j = +1$	$\frac{j}{j+1}$	$\frac{j}{j+1}\frac{m_j+1}{m_j}$	$\frac{j}{j+1}\frac{m_j-1}{m_j}$
$\eta^{a\to a'}$ $\Delta j = -1$	$\frac{j}{j-1}$	$\frac{j}{j-1}\frac{m_j+1}{m_j}$	$\frac{j}{j-1}\frac{m_j-1}{m_j}$
$\eta^{a\to b}$ $\Delta j = 0$	$-\frac{j}{j+1}$	$-\frac{j}{j+1}\frac{m_j+1}{m_j}$	$-\frac{j}{j+1}\frac{m_j-1}{m_j}$
$\eta^{b\to a}$ $\Delta j = 0$	$-\frac{j+1}{j}$	$-\frac{j+1}{j}\frac{m_j+1}{m_j}$	$-\frac{j+1}{j}\frac{m_j-1}{m_j}$
$\eta^{b\to b'}$ $\Delta j = +1$	$\frac{j+1}{j+2}$	$\frac{j+1}{j+2}\frac{m_j+1}{m_j}$	$\frac{j+1}{j+2}\frac{m_j-1}{m_j}$
$\eta^{b\to b'}$ $\Delta j = -1$	$\frac{j+1}{j}$	$\frac{j+1}{j}\frac{m_j+1}{m_j}$	$\frac{j+1}{j}\frac{m_j-1}{m_j}$

momentum quantum number by 1 or $\Delta j = \pm 1$, while the transition between ψ_a and ψ_b does not change j, or $\Delta j = 0$. The spin angular momenta for the above two states are[106]

$$S_z^a = \frac{m_j}{j}\frac{\hbar}{2} \tag{5}$$

$$S_z^b = -\frac{m_j}{j+1}\frac{\hbar}{2}, \tag{6}$$

where we see that ψ_a is mainly in a spin-up state while ψ_b is in a spin-down state, if $m_j > 0$ is assumed.

To quantify the spin reversal, we employ the dimensionless spin switchability

$$\eta = \frac{S_z^f}{S_z^i}, \tag{7}$$

where $S_z^{i(f)}$ is the initial (final) spin. $\eta > 1$ means that the spin increases in the original direction of the initial spin; $1 > \eta \geq 0$ corresponds to the demagnetization; $-1 \leq \eta < 0$ signifies the spin reversal; and $\eta < -1$ indicates that the spin is reversed and increases in the opposite direction of the original spin. Among the linearly and circularly polarized lights, there are 18 possible spin changes. They cover the full spectrum of the spin excitation.

We start with linearly polarized light (LP), where $\Delta m_j = 0$. Table 1 shows that for $\Delta j = +1$, regardless of whether the transition is between ψ_a states or between ψ_b states, η is positive and less than 1, or demagnetization. By contrast, for $\Delta j = -1$, it corresponds to magnetization enhancement since $\eta > 1$. ψ^a and ψ^b each have one demagnetization ($\Delta j = +1$) and one magnetization channel ($\Delta j = -1$) if the transition is only between ψ_a states or ψ_b states. These two channels can not be categorized as a thermal process, since the photon angular momentum is transferred to ($\Delta j = 1$) and away from ($\Delta j = -1$) the system. Quantitatively, η depends on j. For example, consider $\psi_a \to \psi_{a'}$, and with $\Delta j = 1$ (demagnetization), if $j = 3/2$, $\eta = 3/5$, the percentage spin loss is $1 - \eta = 2/5$, or 40%. This means that for a single photon absorbed, the spin can be reduced by 40%, which is compatible

to the experimental findings.[5] When j becomes larger, the loss is smaller. For the spin enhancement ($\Delta j = -1$), we can develop a similar theoretical basis. So far, we have only considered $\Delta j = \pm 1$. $\Delta j = 0$ only occurs for the transition between one ψ^a and one ψ^b state, and leads to the absolute spin reversal. There are two channels, $\psi_a \rightarrow \psi_b$ and $\psi_b \rightarrow \psi_a$. Transitioning from ψ_a to ψ_b switches spin from up to down, while transitioning from ψ_b to ψ_a switches spin from down to up. This simple picture nicely explains why LP creates multiple domains with mixed spin up and spin down.[63] The final outcome, whether it is demagnetization, magnetization or spin reversal, critically depends which transitions dominate.

For left (LC) and right (RC) circularly polarized light, the situation is more complicated since now m_j plays a role. This is reflected in Table 1. However, we find that there is a simple and similar dependence of η on j as LP. If we ignore those m_j terms in η, each of the resultant j terms under LC and RC is exactly the same as LP, comparing column 2 with 3 and column 2 with 4. The magnetic quantum number m_j opens new channels to manipulate spin. For instance, in the second column where the transition is between ψ^a states and $\Delta j = +1$, if $m_j = -1/2$, for LC, $\eta = -j/(j+1) < 0$, corresponding to spin reversal. The same is true for $\Delta j = -1$. In fact, all the six channels are open for spin reversal, in comparison to two channels in LP; the same can be said for magnetization and demagnetization. This explains why LC and RC appear more powerful to switch spins than LP.[74] For RC, the situation is similar if we have $m_j = 1/2$. Our results question again whether it is appropriate to label the helicity-independent switching as thermal switching, since the entire process is still optical.[89]

In the following, we will construct a model to demonstrate that the insight gained from these spin-orbit coupled states is useful and appears in our calculation below.

4.2. *Spin reversal theory: cw limit*

In contrast to the title of this subsection, our original idea was to derive an analytic expression for traditional magneto-optics under cw excitation from a simple model suggested by Bigot[d] to us in 1999. Bigot wondered whether it is possible to develop a simple model to compare the theory with the experimental finding. Note, however, that Pershan *et al.*[96] and others[107] already used the simple oscillator model to compute the magneto-optical response. Common to these theories is that the magnetic field is used, since the classical theory traditionally does not have spin in it. A nice feature of such an approach is that an analytic solution for the diagonal and off-diagonal susceptibilities is possible.

However, we have no prior bias toward the magnetic field, since our prior theoretical investigations[25,108,23] often do not have a magnetic field. So, we simply

[d]Private conversation

replaced the magnetic field by the spin-orbit coupling,[89,109,110,111,112,113]

$$H = \frac{\mathbf{p}^2}{2m} + \frac{1}{2}m\Omega^2\mathbf{r}^2 + \lambda\mathbf{L}\cdot\mathbf{S} - e\mathbf{E}(t)\cdot\mathbf{r}. \tag{8}$$

Here, the first term is the kinetic energy operator of the electron; the second term is the harmonic potential energy operator with system frequency Ω; λ is the spin-orbit coupling in units of eV/$\hbar^2$; $\mathbf{L}$ and $\mathbf{S}$ are the orbital and spin angular momenta in units of $\hbar$, respectively, and $\mathbf{p}$ and $\mathbf{r}$ are the momentum and position operators of the electron, respectively. Note that $\mathbf{L}$ is computed from $\mathbf{L} = \mathbf{r}\times\mathbf{p}$, and there is no need to set up a different equation for it.

The entire equation of motion can be written down as[113]

$$\frac{d\mathbf{r}}{dt} = \frac{\mathbf{p}}{m} - \lambda(\mathbf{r}\times\mathbf{S}), \tag{9}$$

$$\frac{d\mathbf{p}}{dt} = -m\Omega^2\mathbf{r} + e\mathbf{E}(t) - \lambda\mathbf{p}\times\mathbf{S}, \tag{10}$$

$$\frac{d\mathbf{S}}{dt} = \lambda(\mathbf{L}\times\mathbf{S}), \tag{11}$$

$$\frac{d\mathbf{L}}{dt} = -e\mathbf{E}(t)\times\mathbf{r} - \lambda(\mathbf{L}\times\mathbf{S}), \tag{12}$$

where the last equation does not enter the calculation and is left here for later usage. The total angular momentum $\mathbf{J}$ is determined by the laser field and position vector. If we assume that the spin is constant, then three coupled equations (9)-(11) can be simplified as[113]

$$\ddot{\mathbf{r}} + 2\lambda\dot{\mathbf{r}}\times\mathbf{S} + (\Omega^2 - \lambda^2S^2)\mathbf{r} - \lambda^2(\mathbf{r}\cdot\mathbf{S})\mathbf{S} = \frac{e\mathbf{E}(t)}{m}. \tag{13}$$

If the external field is cw, we can derive the susceptibilities analytically as

$$\chi^{(1)}_{xx}(\omega) = -\frac{Ne^2}{\epsilon_0 m}\frac{\Omega^2 - \omega^2 - \lambda^2S_z^2}{(\Omega^2 - \omega^2 - \lambda^2S_z^2)^2 - (2\lambda S_z\omega)^2} \tag{14}$$

$$\chi^{(1)}_{xy}(\omega) = -i\frac{Ne^2}{\epsilon_0 m}\frac{2\lambda S_z\omega}{(\Omega^2 - \omega^2 - \lambda^2S_z^2)^2 - (2\lambda S_z\omega)^2}, \tag{15}$$

where N is the number density and ϵ_0 is the permittivity in vacuum. This result convinces us that the model can describe the basic features of the magneto-optics.

4.3. *Spin reversal theory: pulsed laser*

With the success of our model to describe the basic magneto-optics, we wonder whether such an equation allows us to describe spin switching. It is easy to show from Eq. (11) that the spin is conserved, and its module does not change with time. This indicates that spin switching may be possible.

The key step has been outlined in our study.[113] Here, we give a summarized account. To start with, we solve the equations of motion numerically. We choose laser pulses of two different kinds. For a linearly polarized (π) pulse, the electric

field is $\mathbf{E}(t) = A_0 e^{-t^2/\tau^2} \cos(\omega t)\hat{x}$, where ω is the laser carrier frequency, τ is the laser pulse duration, A_0 is the laser field amplitude, t is time, and $\hat{x}$ is the unit vector along the x axis. Note that the results are the same if the field is along the y axis. The electric field for the right- and left-circularly polarized pulses (σ^+ and σ^-) is $\mathbf{E}(t) = A_0 e^{-t^2/\tau^2}(\pm \sin(\omega t)\hat{x} + \cos(\omega t)\hat{y})$, where $+(-)$ refers to $\sigma^+(\sigma^-)$. We then compute the spin evolution by numerically solving the three coupled equations (9-11). Since we did not know whether the spin momentum has any major effect on the spin reversal, we choose the initial spin momentum $S_z(0) = 2.2\hbar$. It turns out that this is a crucial step. Had we chosen a smaller value, we could miss the spin reversal entirely since too small a spin could not reverse the spin, regardless of the laser field amplitude. We choose the spin-orbit coupling $\lambda = 0.06\text{eV}/\hbar^2$, and $\hbar\omega = \hbar\Omega = 1.6$ eV. This is a resonant excitation. If we have an off-resonant excitation, the spin can not be switched over effectively. For this reason, our theory is based on photon absorption, or photomagnetism. Our pulse duration is $\tau = 60$ fs and amplitude is 0.035 V/Å, which is already optimized. We also assume that the electron moves along the z axis with velocity 1 Å/fs or 10^5 m/s, which is slightly lower than the Fermi velocity. We find that this initial velocity is necessary due to the uncertainty principle; otherwise, since the laser field is only in the xy plane, the electron only moves in the xy plane, and there is no way to have a nonzero orbital angular momentum along the x or y axis, so the term on the left-hand side of Eq. (11) is zero. A larger value of v_z leads to a larger effect in the spin reversal. Here, we want to be conservative, so we choose a smaller value. The initial values of v_x and v_y do not matter too much since the laser is in the xy plane anyway.

Figure 7(a) shows the spin reversal on this single site. We initialize the spin along the $-z$ axis. Upon the laser excitation, the spin first precesses strongly without any oscillation toward the xy plane, and the exact precession of S_x and S_y depends on the initial phase of the laser pulse,[e] but the precession of S_z is always the same. The spin reaches the negative maximum at 34 fs, exactly when S_z passes through zero. S_z successfully switches to $2\hbar$ at 80 fs, where the spin rotates 155.9°. Figure 7(b) shows that both σ^+ and σ^- can switch spin within a few hundred femtoseconds. Our results reveal a stringent symmetry constraint on the spin switching: the σ^- light only switches the spin from down to up, while the σ^+ light switches the spin from up to down, not the other way around. We have also tested the linearly polarized light. We find that depending on the initial spin orientation, LP can switch from down to up and from up to down (see Fig. 7(c)). More importantly, the needed laser amplitude is much larger. To induce spin switching, we need to increase A_0 above 0.2V/Å, or 5.7 times higher than that used for either σ^+ or σ^-. This result is consistent with the finding by Alebrand *et al.*[74]

Vahaplar *et al.*[68] found that AOS does not occur with any laser field fluence.

[e]Our current integration starts at -1000 fs, where the amplitude of the laser field is extremely small. If we change it to a different time, then S_x and S_y may behave differently, depending on the initial phase that the laser acquires. However, S_z remains the same.

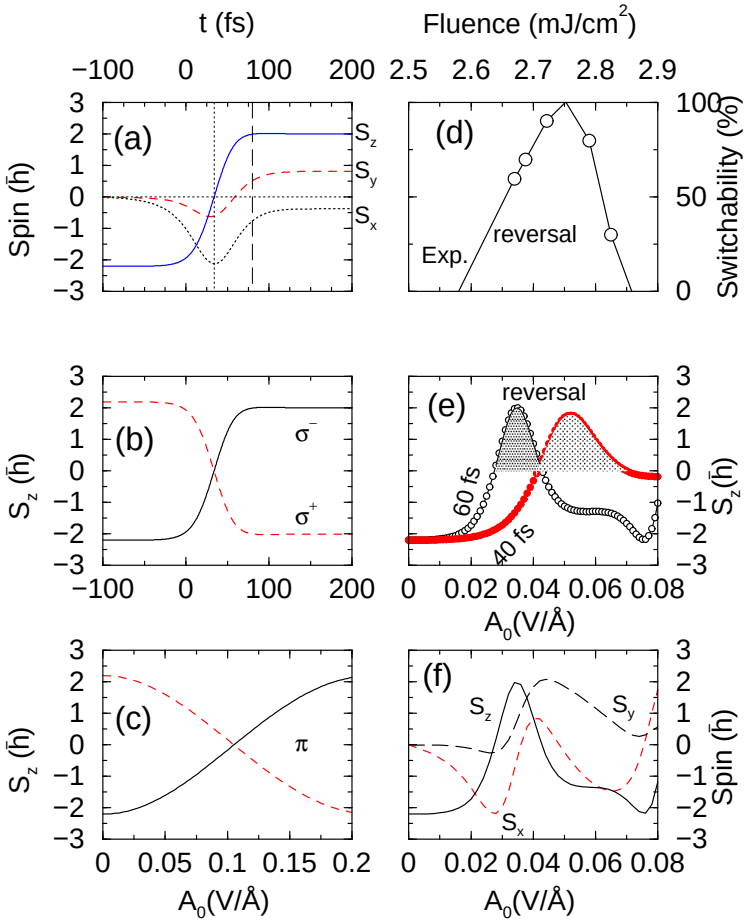

Fig. 7. (a) All-optical spin reversal for S_x, S_y and S_z as a function of time t. The vertical dotted line denotes the time when S_z passes through zero, and the vertical dashed line denotes the time when the spin reversal starts. Here σ^- is used, the laser pulse duration is $\tau = 60$ fs, and the field amplitude is 0.035 V/Å. (b) The σ^- pulse (solid line) only switches spin from down to up, while the σ^+ pulse (dashed line) only switches spin from up to down. (c) The π pulse can switch spin from up to down or from down to up, but at a much higher field amplitude. (d) Experimental spin reversal window from Ref. 28. (e) Final spin angular momentum S_z as a function of the laser field amplitude for laser duration $\tau = 60$ fs (empty circles) and 40 fs (filled red circles). The shaded regions are the spin reversal window. (f) As the field amplitude increases, the spin angular momentum changes from non-switching, canting along the $-x$ axis, switching, and canting along the $+y$ axis. The figure is from Ref. 112 used with permission from EPL.

They discovered that the spin reversal window is very narrow and asymmetric (see Fig. 7(d)). Our theoretical results are shown in Fig. 7(e). We see that as A_0 increases, the final spin S_z first increases sharply (see the empty circles) and then reaches its maximum of $2\hbar$ at $A_0 = 0.035$V/Å, where the spin is reversed. If we

increase the field amplitude further, S_z decreases, and eventually the spin switching disappears. The reversal window is indeed very narrow and asymmetric (see the shaded region in Fig. 7(b)), only from 0.026 to 0.042 V/Å.

It is interesting to investigate how the spin changes for those unoptimized amplitudes. For this, we plot all three components of the spin as a function of the laser field amplitude. It is clear that when the amplitude is small, the spin change is small. But as we gradually increase it to about 0.026 V/Å, the final spin simply cants along the $-x$ axis. On the other hand, if we have too big an amplitude above 0.035 V/Å but below 0.06 V/Å, the spin cants to the $+y$ axis. Therefore, a competition between spin canting and spin reversal leads to the asymmetric dependence of the switchability on the laser amplitude. We find a better agreement with the experimental one[68] than their own theoretical results. This is the first indication that our theory may catch something important here.

4.4. *Exchange interaction and Rise of inverse Faraday effect*

However, Vahaplar *et al.*[68] included the exchange interaction between different spins and their system is much larger than ours. In our case, we basically have a single site. To properly include the exchange coupling, we construct the following Hamiltonian [110,89]

$$H = \sum_i \left[\frac{\mathbf{p}_i^2}{2m} + V(\mathbf{r}_i) + \lambda \mathbf{L}_i \cdot \mathbf{S}_i - e\mathbf{E}(\mathbf{r}, t) \cdot \mathbf{r}_i \right] - \sum_{ij} J_{ex} \mathbf{S}_i \cdot \mathbf{S}_j. \tag{16}$$

The summation is over all the lattice sites. Here, the first four terms are the same as our Hamiltonian (8). The last term is the exchange interaction, and J_{ex} is the exchange integral in units of eV/$\hbar^2$. Such a Hamiltonian contains the necessary ingredients for AOS; a similar form is often used for magnetic multilayers.[114,115]

We consider a slab of $101 \times 101 \times 4$ lattice sites, where we can shed some new light on the inverse Faraday effect. We take $S(0)_z = 1.2\hbar$ as an example. The field amplitude is at its optimal value of $A_0 = 0.018$ V/Å. As stated above, the orbital angular momentum evolves with time according to

$$\frac{d\mathbf{L}_i}{dt} = -e\mathbf{E}(t) \times \mathbf{r}_i - \lambda(\mathbf{L}_i \times \mathbf{S}_i). \tag{17}$$

The two driving terms on the right-hand side represent two torques. The first term is the torque due to the laser field, $\tau_{laser} = -e\mathbf{E}(t) \times \mathbf{r}_i$. Note that here τ is the torque, not to be confused with the duration above. This is a cross-product of the laser field and electron position, not that of the field and itself, which is in sharp contrast to Eq. (2) under cw excitation. Our finding is also consistent with the study by Popova *et al.*,[94] where the effective field is not a simple product of two fields. Different from Popova *et al.*, our effective field acts upon the orbital angular momentum, not spin. If we directly compute the spin momentum change, the net change in the module is small, but the spin precesses very strongly.

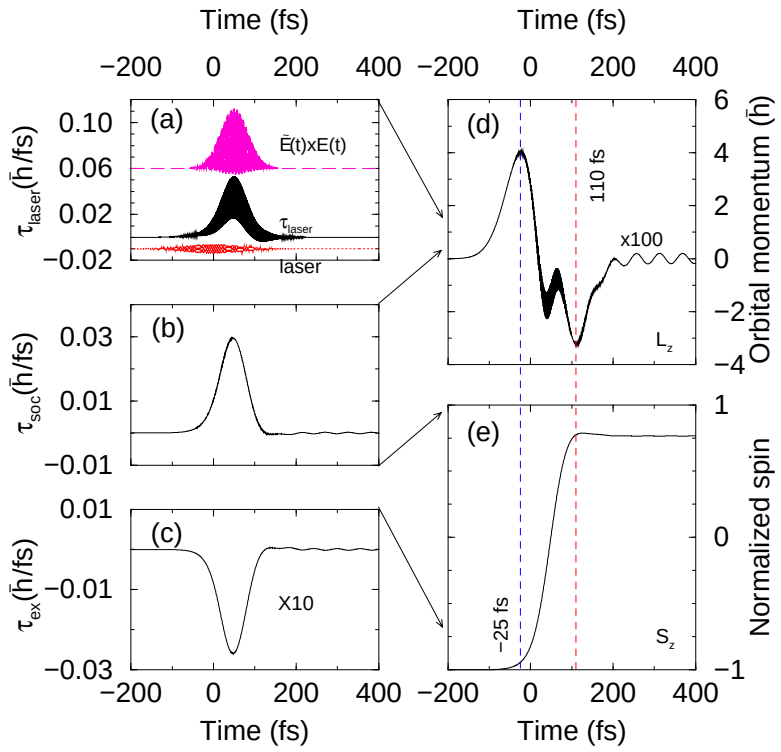

Fig. 8. (a) Laser-induced torque τ_{laser} as a function of time. The peak is at 50 fs, different from the laser field (see the bottom curve) peak at 0 fs. The long-dashed line refers to the effective field computed from $\tilde{\mathbf{E}}(t)\times\mathbf{E}(t)$. Here $S_z(0) = 1.2\hbar$. (b) Spin-orbit torque change τ_{soc} with time. This is the main torque to reverse the spin. (c) Exchange-interaction torque change τ_{ex} with time. It is at least 10 times smaller than the spin-orbit torque. (d) Orbital angular momentum L_z as a function of time. It peaks at -25 fs, which is ahead of spin reversal by 135 fs. The first vertical dashed line refers to the peak time. (e) Spin reversal. The spin is initialized along the $-z$ direction, and upon laser excitation, the spin is reversed to the $+z$ direction around 110 fs. The spin is normalized with respect to the initial spin $S_z(0) = 1.2\hbar$.

The solid curve in Fig. 8(a) shows the z component of τ_{laser}, while the dotted curve is our laser E-field. It is clear that τ_{laser} is quite different from the laser pulse itself: (i) it peaks at 50 fs, not 0 fs; (ii) it is asymmetric; and (iii) its values are mostly positive. However, if we assume that the position behaves like $|\tilde{\mathbf{E}}(t)| \propto \cos(\omega t + \pi/5)\exp(-(t-54)^2/64.7^2)$, τ_{laser} can be reproduced to some extent by $\tilde{\mathbf{E}}(t) \times \mathbf{E}(t)$ (see the long dashed line). This reminds us of the inverse Faraday effect,[7] but this cross product provides a source term for the electron orbital angular momentum, not for the spin.[63,66,79] From Eq. (17), we see that τ_{laser} is not the only torque that affects the orbital. Once the orbital angular momentum differs from zero, $\tau_{soc} = -\lambda \mathbf{L}_i \times \mathbf{S}_i$ builds up and starts to contribute a negative torque to the orbital angular momentum (see Fig. 8(b)). Figure 8(c) shows that the exchange

torque τ_{ex} is at least one order of magnitude weaker than τ_{soc}, so τ_{soc} dominates over τ_{ex}.

Figure 8(d) shows that upon laser excitation, the orbital angular momentum L_z in the first layer of atomic sites increases sharply from $0.0\hbar$ to $0.04\hbar$ at -25 fs, after which it swings to the negative maximum of $-0.03\hbar$ before it returns to zero and oscillates around it. Other layers have a similar dependence (not shown). A competition between τ_{laser} and τ_{soc} leads to a sudden reduction of L_z around 18 fs and subsequent reversal at 110 fs, which explains the violent oscillation in L_z (see Fig. 8(d)). The change in spin is quite different. Figure 8(e) shows that the normalized spin starts from -1 and flips over to 0.75 at 110 fs. The spin dynamics delays with respect to the orbital dynamics by 135 fs. The peak of τ_{soc} corresponds to the maximum change in S_z, while the small value of τ_{soc} after the peak ensures that the spin can not be switched back. τ_{soc} provides a necessary positive torque that finally flips the spin from the $-z$ to $+z$ direction.

4.5. *Effect of the laser field amplitude on spin reversal*

We have already seen how the laser field amplitude affects spin reversal at a single site. Here we have a much larger system. To reveal further insight into the effect of the laser field amplitude on spin reversal, we choose three amplitudes, $A_0 = 0.014$, 0.018 and 0.022 V/Å, and $S_z(0) = 1.2\hbar$. We take the first layer as an example, since the rest of them behave similarly except for a slight time delay. The spin configuration is initialized along the $-z$ axis (see the light blue arrows in Figs. 9(a-c)). We start with $A_0 = 0.014$ V/Å. We find that as time evolves, the spin does try to flip, but the final spin only tilts toward the yz plane, and it does not have enough power to reach the full reversed spin configuration. If we increase the amplitude to $A_0 = 0.018$ V/Å, we see from Fig. 9(b) that the spin is capable of flipping into the opposite direction. Now if we increase the laser amplitude further to $A_0 = 0.022$ V/Å, the situation changes. Figure 9(c) shows that the spin rotates too much; and once the field is off, it cants toward the xy plane.

The above field dependence can be understood from the spin-orbit torque. Figures 9(d-f) show the respective three-dimensional torques for each amplitude. Note that all the torques in the figure are in the units of $\hbar$/fs. Since our initial spin is in the $-z$ direction and our desired final spin is in the $+z$ direction, the torque has to be positive and must be dominated by the z component; otherwise, we only see the spin canting, not switching. Figure 9(d) shows that the torque starts from 0 and gradually grows. It is positive, but the amplitude is small only around 0.01 $\hbar$/fs, which explains why the spin can not be switched over. At $A_0 = 0.018$ V/Å, the torque is positive and larger than that at $A_0 = 0.014$ V/Å. This is the origin of the spin reversal. If the field amplitude is increased to $A_0 = 0.022$ V/Å, the situation in the earlier stage is similar to that at $A_0 = 0.018$ V/Å, but since the amplitude is larger, the torque is larger. As time evolves, it precedes to a negative value of -0.02 $\hbar$/fs. This proves to be detrimental to the spin reversal, which explains why

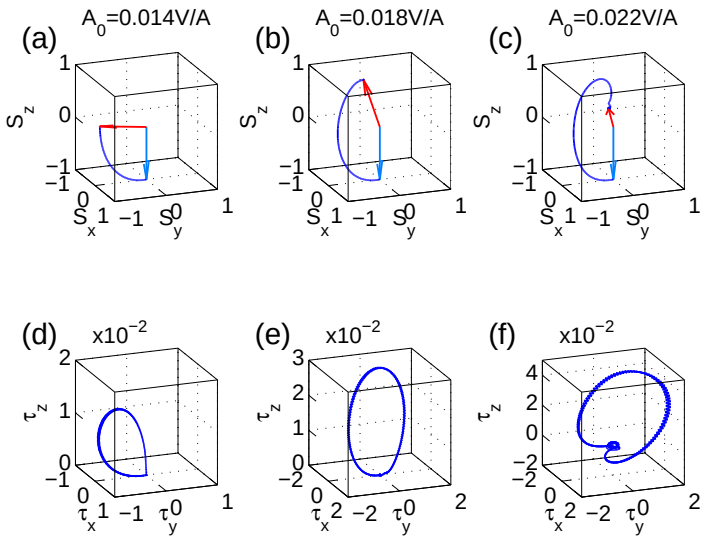

Fig. 9. Effect of the laser field amplitude on spin reversal. (a) Three-dimensional spin precession for the field amplitude $A_0 = 0.014$ V/Å. Here $S_z(0) = 1.2\hbar$. The spin is initiated along the $-z$ axis (see the blue arrow). The red arrow denotes the final spin. All the spins are normalized. (b) Same as (a) but with field amplitude $A_0 = 0.018$ V/Å. Here the spin does reverse successfully. (c) Same as (a) but with field amplitude $A_0 = 0.022$ V/Å. Here the spin passes the optimal location. (d) Three-dimensional plot of the spin-orbit torque τ_{soc} for $A_0 = 0.014$ V/Å. It is mostly positive but small. All the torques are multiplied by 100 for easy viewing and are in the units of $\hbar$/fs. (e) Same as (d), but with $A_0 = 0.018$ V/Å. This is the case that the torque is big and positive. (f) Same as (d), but with $A_0 = 0.022$ V/Å. In the beginning of the laser excitation, this torque is big and positive, but at the end, becomes negative. This forces the spin away from the $+z$ axis.

the final spin passes the optimal configuration. To summarize, to reverse spins, the laser field amplitude has to be in the narrow region, where the spin-orbit torque is not too small, and not too big to turn negative. This competition leads to a narrow region, as seen in experiments.[66]

5. New techniques and new directions

He *et al.*[116] demonstrated AOS using a telecom-band femtosecond fiber laser, and then they fabricated Hall cross devices that can read out the AOS signal by measuring the anomalous Hall voltage changes. Such an incredible technique becomes very useful to characterize AOS switching.[75,76] The amorphous TbFeCo thin films also show bistable magneto-resistance states.[117] Such an exchange bias device can perform even at room temperature.

El Hadri *et al.*[76] directly applied the ferromagnetic Hall crosses[116] to character-

ize the AOS in ferromagnetic Pt/Co/Pt heterostructures. AOS is measured through the anomalous Hall effect. Such a technique provides an alternative to the magnetic imaging technique. They found that the AOS in Pt/Co/Pt is a cumulative process, where a certain number of optical pulses is necessary to obtain full and reproducible switching. This finding was also found in granular FePt by Takahashi *et al.*[118] This is quite different from AOS in GdFeCo.[75] They suggested this could become a new type of opto-spintronic device. Such an idea could be incorporated with electric switching, such as the recently demonstrated switching in CuMnAs.[119]

In 2015, Satoh *et al.*[120] demonstrated that an arbitrary optical polarization write/read is possible in antiferromagnet $YMnO_3$. This idea is consistent with the theoretical prediction by Gomez-Abal *et al.*[121] However, the entire process is a rapid beating and does not settle down to a definitive state. This potentially will limit its application, if used as a switching device.

Ogawa *et al.*[122] studied the local excitation of the spin in magnetic skyrmions Cu_2OSeO_3. They showed that the spins in the conical and skyrmions phases can be excited by the effective impulsive magnetic field from the inverse-Faraday effect. It would be interesting if the spin could be permanently switched.

Very recently, Goncalves *et al.*[123] demonstrated that a sub-10-fs pulse is able to efficiently excite a magnetic system such as GdFeCo. This revealed unprecedented details on the electron-electron interaction time scale. Note that all the previous investigations were carried out over tens of femtoseconds.[63] It is likely that the observed picosecond spin reversal in fact starts earlier. It is the current magnetic image techniques that limit our view on the shortest possible time scale.

6. Conclusions

We have presented a short review on all-optical spin switching and a simple model that works quite well to explain all-optical helicity-dependent spin switching (AOS). To give the reader a complete picture of AOS, we have discussed the initial phase of femtomagnetism with emphasis on ultrafast demagnetization. Then we focus on the experimental discovery of AOS as a major branch of femtomagnetism. AOS is an extremely active research area at this time. The new theoretical and experimental findings are reported frequently. It is impossible to include all aspects of the current research, so we limit our focus to four major directions of the experimental discoveries: (1) temperature effect; (2) laser parameter effect; (3) effect of the sample composition; and (4) AOS samples beyond GdFeCo.

Before we turn to our latest research on AOS at a single spin site, we show that a simple all-optical spin switching rule exists, and it provides essential guidance as to how microscopically the light reverses the spin and how the light helicity affects the AOS. We find that although our spin-orbit coupled harmonic model is very simple, it contains some important elements for magneto-optics and all-optical spin switching. Even in the static limit, we show that the simple model reproduces the well-known dependence of the diagonal and off-diagonal susceptibility on the

spin angular momentum and spin-orbit coupling. We show numerically that spin reversal is possible within such a model. The results are very good. For instance, they match the experimental laser fluence dependence, even better than other more complicated models. Even more interesting is that our model reveals that the spin-orbit torque plays the role as an effective magnetic field, an equivalent field to the inverse Faraday effect, which has long been sought after.

In summary, additional experimental and theoretical work is necessary to iron out the details of the complicated underlying mechanism of the all-optical switching. On the theoretical side, at present, the theoretical efforts largely follow the experimental development. There have been very few predictions, partly because the majority of the theories are heavily phenomenological and empirical. There is a need to include true laser pulses, not heat pulse or effective magnetic field. Much fewer studies are in the structural study. This is a new direction that is going to be important in the future. Experimentally, pursuing a simpler system, as a way to understanding the complex rare-earth compounds, is very helpful. This should be coupled with the element-specific technique, so one can be sure which spin and which element is switched. A systematic investigation of the composition is needed. We think that this is the single most important addition to AOS. A joint effort between theory and experiment is expected to yield new and more exciting results, and possibly open new applications in femtomagnetism.

Acknowledgments

This work was solely supported by the U.S. Department of Energy under Contract No. DE-FG02-06ER46304. Part of the work was done on Indiana State University's quantum cluster and high-performance computers. The research used resources of the National Energy Research Scientific Computing Center, which is supported by the Office of Science of the U.S. Department of Energy under Contract No. DE-AC02-05CH11231. This work was performed, in part, at the Center for Integrated Nanotechnologies, an Office of Science User Facility operated for the U.S. Department of Energy (DOE) Office of Science by Los Alamos National Laboratory (Contract DE-AC52-06NA25396) and Sandia National Laboratories (Contract DE-AC04-94AL85000).

References

1. H. P. D. Shieh and M. H. Kryder, Appl. Phys. Lett. **49**, 473 (1986).
2. A. Aharoni, *Introduction to the Theory of Ferromagnetism*, 2nd Ed. (Oxford Science Publications, 2000), p. 128.
3. A. Vaterlaus, T. Beutler, and F. Meier, Phys. Rev. Lett. **67**, 3314 (1991).
4. W. Hübner and K. H. Bennemann, Phys. Rev. B **53**, 3422 (1996).
5. E. Beaurepaire, J. C. Merle, A. Daunois, and J.-Y. Bigot, Phys. Rev. Lett. **76**, 4250 (1996).
6. G. P. Zhang, W. Hübner, E. Beaurepaire, and J.-Y. Bigot, Topics Appl. Phys. **83**, 245 (2002).

7. A. Kirilyuk, A. V. Kimel, and Th. Rasing, Rev. Mod. Phys. **82**, 2731 (2010).
8. A. Kirilyuk *et al.*, Rep. Prog. Phys. **76**, 026501 (2013).
9. A. Kirilyuk *et al.*, Low Temp. Phys. **32**, 748 (2006).
10. B. Hillebrands and K. Ounadjela, *Spin Dynamics in Confined Magnetic Structures I* (Springer-Verlag, Berlin/Heidelberg/New York, 2002).
11. B. Hillebrands and K. Ounadjela, *Spin Dynamics in Confined Magnetic Structures II* (Springer-Verlag, Berlin/Heidelberg/New York, 2003).
12. B. Hillebrands and A. Thiaville, *Spin Dynamics in Confined Magnetic Structures III* (Springer-Verlag, Berlin/Heidelberg/New York, 2006).
13. J. Stöhr and H. C. Siegmann, *Magnetism: From Fundamentals to Nanoscale Dynamics* (Springer-Verlag, Berlin/Heidelberg/New York, 2006).
14. J.-Y. Bigot, W. Hübner, Th. Rasing, and R. Chantrell, Eds. *Ultrafast Magnetism I*, Springer Proceedings in Physics **159** (2015).
15. A. Scholl, L. Baumgarten, R. Jacquemin, and W. Eberhardt, Phys. Rev. Lett. **79**, 5146 (1997).
16. J. Hohlfeld, E. Matthias, R. Knorren, and K. H. Bennemann, Phys. Rev. Lett. **78**, 4861 (1997).
17. M. Aeschlimann, M. Bauer, S. Pawlik, W. Weber, R. Burgermeister, D. Oberli, and H. C. Siegmann, Phys. Rev. Lett. **79**, 5158 (1997).
18. C. La-O-Vorakiat, M. Siemens, M. M. Murnane, H. C. Kapteyn, S. Mathias, M. Aeschlimann, P. Grychtol, R. Adam, C. M. Schneider, J. M. Shaw, H. Nembach, and T. J. Silva, Phys. Rev. Lett. **103**, 257402 (2009).
19. B. Koopmans, M. van Kampen, J. T. Kohlhepp, and W. J. M. de Jonge, Phys. Rev. Lett. **85**, 844 (2000).
20. L. Guidoni, E. Beaurepaire, and J.-Y. Bigot, Phys. Rev. Lett. **89**, 017401 (2002).
21. J.-Y. Bigot, L. Guidoni, E. Beaurepaire, and P. Saeta, Phys. Rev. Lett. **93**, 077401 (2004).
22. M. Vomir, L. Andrade, L. Guidoni, E. Beaurepaire, and J.-Y. Bigot, Phys. Rev. Lett. **94**, 237601 (2005).
23. G. P. Zhang, W. Hübner, G. Lefkidis, Y. Bai, and T. F. George, Nature Phys. **5**, 499 (2009).
24. H. Regensburger, R. Vollmer, and J. Kirschner, Phys. Rev. B **61**, 14716 (2000).
25. G. P. Zhang and W. Hübner, Phys. Rev. Lett. **85**, 3025 (2000).
26. G. Ju, A. Nurmikko, R. Farrow, R. Marks, M. Carey, and B. Gurney, Phys. Rev. Lett. **82**, 3705 (1999).
27. T. Kise, T. Ogasawara, M. Ashida, Y. Tomioka, Y. Tokura, and M. Kuwata-Gonokami Phys. Rev. Lett. **85**, 1986 (2000).
28. Q. Zhang, A. Nurmikko, A. Anguelouch, G. Xiao, and A. Gupta, Phys. Rev. Lett. **89**, 177402 (2002).
29. G. M. Müller, J. Walowski, M. Djordjevic, G.-X. Miao, A. Gupta, A. V. Ramos, K. Gehrke, V. Moshnyaga, K. Samwer, J. Schmalhorst, A. Thomas, A. Hütten, G. Reiss, J. S. Moodera, and M. Münzenberg, Nat. Mater. **8**, 56 (2009).
30. A. Kimel, R. Pisarev, J. Hohlfeld, and Th. Rasing, Phys. Rev. Lett. **89**, 287401 (2002).
31. H.-S. Rhie, H. Dürr, and W. Eberhardt, Phys. Rev. Lett. **90**, 247201 (2003).
32. R. Gomez-Abal, O. Ney, K. Satitkovitchai, and W. Hübner, Phys. Rev. Lett. **92**, 227402 (2004).
33. N. Duong, T. Satoh, and M. Fiebig, Phys. Rev. Lett. **93**, 117402 (2004).
34. T. Satoh, S.-J. Cho, R. Iida, T. Shimura, K. Kuroda, H. Ueda, Y. Ueda, B. A. Ivanov, F. Nori, and M. Fiebig, Phys. Rev. Lett. **105**, 077402 (2010).
35. J. Wang, C. Sun, J. Kono, A. Oiwa, H. Munekata, L. Cywinski, and L. J. Sham, Phys.

Rev. Lett. **95**, 167401 (2005).
36. J. Wang, I. Cotoros, K. Dani, X. Liu, J. Furdyna, and D. Chemla, Phys. Rev. Lett. **98**, 217401 (2007).
37. C. Stamm, T. Kachel, N. Pontius, R. Mitzner, T. Quast, K. Holldack, S. Khan, C. Lupulescu, E. F. Aziz, M. Wietstruk, H. A. Dürr, and W. Eberhardt, Nat. Mater. **6**, 740 (2007).
38. B. Koopmans, G. Malinowski, F. Dalla Longa, D. Steiauf, M. Fähnle, T. Roth, M. Cinchetti, and M. Aeschlimann, Nat. Mater. **9**, 259 (2009).
39. K. Carva, M. Battiato, and P. M. Oppeneer, Phys. Rev. Lett. **107**, 207201 (2011).
40. B. Y. Mueller, A. Baral, S. Vollmar, M. Cinchetti, M. Aeschlimann, H. C. Schneider, and B. Rethfeld, Phys. Rev. Lett. **111**, 167204 (2013).
41. S. Bonetti, M. C. Hoffmann, M.-J. Sher, Z. Chen, S.-H. Yang, M. Samant, S. S. P. Parkin, H. A. Dürr, arXiv:1604.04077.
42. T. Tsatsoulis, C. Illg, M. Haag, B. Y. Mueller, L. Zhang, and M. Fähnle, Phys. Rev. B **93**, 134411 (2016).
43. G. Lefkidis and W. Hübner, J. Mag. Mag. Mater. **321**, 979 (2009).
44. L. Andrade, A. Laraoui, M. Vomir, D. Muller, J.-P. Stoquert, C. Estourns, E. Beaurepaire, and J.-Y. Bigot, Phys. Rev. Lett. **97**, 127401 (2006).
45. M. Pickel, A. Schmidt, F. Giesen, J. Braun, J. Minr, H. Ebert, M. Donath, and M. Weinelt, Phys. Rev. Lett. **101**, 066402 (2008).
46. G. P. Zhang, Phys. Rev. Lett. **101**, 187203 (2008).
47. A. B. Schmidt, M. Pickel, M. Donath, P. Buczek, A. Ernst, V. P. Zhukov, P. M. Echenique, L. M. Sandratskii, E. V. Chulkov, and M. Weinelt, Phys. Rev. Lett. **105**, 197401 (2010).
48. M. Battiato, K. Carva, and P. M. Oppeneer, Phys. Rev. Lett. **105**, 027203 (2010).
49. D. Rudolf, C. La-O-Vorakiat, M. Battiato, R. Adam, J. M. Shaw, E. Turgut, P. Maldonado, S. Mathias, P. Grychtol, H. T. Nembach, T. J. Silva, M. Aeschlimann, H. C. Kapteyn, M. M. Murnane, C. M. Schneider, and P. M. Oppeneer, Nat. Comms. **3**, 1037 (2012).
50. A. Eschenlohr, M. Battiato, P. Maldonado, N. Pontius, T. Kachel, K. Holldack, R. Mitzner, A. Föhlisch, P. M. Oppeneer and C. Stamm, Nat. Mater. **12**, 332 (2013).
51. B. Vodungbo *et al.*, Scientific Reports **6**, 18970 (2016).
52. E. Turgut, C. La-o-vorakiat, J. M. Shaw, P. Grychtol, H. T. Nembach, D. Rudolf, R. Adam, M. Aeschlimann, C. M. Schneider, T. J. Silva, M. M. Murnane, H. C. Kapteyn, and S. Mathias, Phys. Rev. Lett. **110**, 197201 (2013).
53. A. J. Schellekens, W. Verhoeven, T. N. Vader, and B. Koopmans, Appl. Phys. Lett. **102**, 252408 (2013).
54. M. Lisowski, P. Loukakos, A. Melnikov, I. Radu, L. Ungureanu, M. Wolf, and U. Bovensiepen, Phys. Rev. Lett. **95**, 137402 (2005).
55. A. Melnikov, H. Prima-Garcia, M. Lisowski, T. Gieel, R. Weber, R. Schmidt, C. Gahl, N. Bulgakova, U. Bovensiepen, and M. Weinelt, Phys. Rev. Lett. **100**, 107202 (2008).
56. I. Radu, G. Woltersdorf, M. Kiessling, A. Melnikov, U. Bovensiepen, J.-U. Thiele, and C. H. Back, Phys. Rev. Lett. **102**, 117201 (2009).
57. M. Wietstruk, A. Melnikov, C. Stamm, T. Kachel, N. Pontius, M. Sultan, C. Gahl, M. Weinelt, H. A. Dürr, and U. Bovensiepen, Phys. Rev. Lett. **106**, 127401 (2011).
58. R. Carley, K. Döbrich, B. Frietsch, C. Gahl, M. Teichmann, O. Schwarzkopf, P. Wernet, and M. Weinelt, Phys. Rev. Lett. **109**, 057401 (2012).
59. B. Frietsch, J. Bowlan, R. Carley, M. Teichmann, S. Wienholdt, D. Hinzke, U. Nowak, K. Carva, P. M. Oppeneer, and M. Weinelt, Nat. Commun. **6**, 8262 (2015).
60. J.-W. Kim, M. Vomir, and J.-Y. Bigot, Phys. Rev. Lett. **109**, 166601 (2012).

61. K. Krieger, J. K. Dewhurst, P. Elliott, S. Sharma, and E. K. U. Gross, J. Chem. Theory and Comput. **11**, 4870 (2015).
62. G. P. Zhang, Y. H. Bai and T. F. George, J. Phys.: Condens. Mat. **27**, 236004 (2016).
63. C. D. Stanciu, F. Hansteen, A. V. Kimel, A. Kirilyuk, A. Tsukamoto, A. Itoh, and Th. Rasing, Phys. Rev. Lett. **99**, 047601 (2007).
64. M. Mansuripur, *The Physical Principles of Magneto-Optical Recording* (Cambridge University Press, Cambridge, 1997).
65. R. C. Taylor and A. Gangulee, Phys. Rev. B **22**, 1320 (1980).
66. K. Vahaplar *et al.*, Phys. Rev. B **85**, 104402 (2012).
67. J. Hohlfeld, C. D. Stanciu and A. Rebei, App. Phys. Lett. **94**, 152504 (2009).
68. K. Vahaplar *et al.*, Phys. Rev. Lett. **103**, 117201 (2009).
69. A. Hassdenteufel *et al.*, Adv. Mater. **25**, 3122 (2013).
70. Z. Chen, R. Gao, Z. Wang, C. Xu, D. Chen, and T. S. Lai, J. App. Phys. **108**, 023902 (2010).
71. C. D. Stanciu, A. Tsukamoto, A. V. Kimel, F. Hansteen, A. Kirilyuk, A. Itoh, and Th. Rasing, Phys. Rev. Lett. **99**, 217204 (2007).
72. A. R. Khorsand, M. Savoini, A. Kirilyuk, A. V. Kimel, A. Tsukamoto, A. Itoh, and Th. Rasing, Phys. Rev. Lett. **108**, 127205 (2012).
73. D. Steil, S. Alebrand, A. Hassdenteufel, M. Cinchetti and M. Aeschlimann, Phys. Rev. B **84**, 224408 (2011).
74. S. Alebrand, A. Hassdenteufel, D. Steil, M. Cinchetti, and M. Aeschlimann, Phys. Rev. B **85**, 092401 (2012).
75. M. S. El Hadri, P. Pirro, C. H. Lambert, S. Petit-Watelot, Y. Quessab, M. Hehn, F. Montaigne, G. Malinowski, and S. Mangin, arXiv: 1602.08525v1 (2016).
76. M. S. El Hadri, P. Pirro, C.-H. Lambert, N. Bergeard, S. Petit-Watelot, M. Hehn, G. Malinowski, F. Montaigne, Y. Quessab, R. Medapalli, E. E. Fullerton, and S. Mangin, Appl. Phys. Lett. **108**, 092405 (2016).
77. Ph. Kurz, G. Bihlmayer and S. Blügel, J. Physics.: Condens. Matter **14**, 6353 (2002).
78. J. Jensen and A. R. Mackintosh, *Rare Earth Magnetism: Structures and Excitations* (Clarendon, Oxford, 1991).
79. T. A. Ostler *et al.*, Nat. Commun. **3**, 666 (2012).
80. S. Alebrand *et al.*, Appl. Phys. Lett. **101**, 162408 (2012).
81. S. Alebrand *et al.*, Phys. Rev. B **89**, 144404 (2014).
82. I. Radu, K. Vahaplar, C. Stamm, T. Kachel, N. Pontius, H. A. Dürr, T. A. Ostler, J. Barker, R. F. L. Evans, R. W. Chantrell, A. Tsukamoto, A. Itoh, A. Kirilyuk, Th. Rasing and A. V. Kimel, Nature **472**, 205 (2011).
83. A. R. Khorsand, M. Savoini, A. Kirilyuk, A.V. Kimel, A. Tsukamoto, A. Itoh, and Th. Rasing, Phys. Rev. Lett. **110**, 107205 (2013).
84. S. Mangin *et al.*, Nature Mater. **13**, 286 (2014).
85. C.-H. Lambert *et al.*, Science **345**, 1337 (2014).
86. T. D. Cornelissen, R. Cardoba, and B. Koopmans, Appl. Phys. Lett. **108**, 142405 (2016).
87. J. Gorchon, Y. Yang and J. Bokor, arXiv: 1604.06441v1 (2016).
88. A. Hassdenteufel *et al.*, Optics Express **22**, 10017 (2014).
89. G. P. Zhang and T. F. George, J. Phys.: Condens. Mat. **25**, 366002 (2013).
90. C. Schubert, A. Hassdenteufel, P. Matthes, J. Schmidt, M. Helm, R. Bratschitsch, and M. Albrecht, Appl. Phys. Lett. **104**, 082406 (2014).
91. A. Hassdenteufel *et al.*, Phys. Rev. B **91**, 104431 (2015).
92. J. Barker, U. Atxitia, T. A. Ostler, O. Hovorka, O. Chubykalo-Fesenko and R. W. Chantrell, Scientific Reports **3**, 3262 (2013).

93. V. N. Gridnev, Phys. Rev. B **77**, 094426 (2008).
94. D. Popova, A. Bringer, and S. Blügel, Phys. Rev. B **85**, 094419 (2012).
95. G. Lefkidis, G. P. Zhang and W. Hübner, Phys. Rev. Lett. **103**, 217401 (2009).
96. P. S. Pershan, J. P. van der Ziel, and L. D. Malmstrom, Phys. Rev. **143**, 574 (1966).
97. M. Battiato, G. Barbalinardo and P. M. Oppeneer, Phys. Rev. B **89**, 014413 (2014).
98. V. N. Gridnev, Phys. Rev. B **88**, 014405 (2013).
99. T. A. Ostler, R. F. L. Evans, R. W. Chantrell, U. Atxitia, O. Chubykalo-Fesenko, I. Radu, R. Abrudan, F. Radu, Arata Tsukamoto, A. Itoh, A. Kirilyuk, Th. Rasing, and A. Kimel, Phys. Rev. B **84**, 024407 (2011).
100. V. I. Belotelov and A. K. Zvezdin, Phys. Rev. B **86**, 155133 (2012).
101. S. Wienholdt, D. Hinzke, K. Carva, P. M. Oppeneer, and U. Nowak, Phys. Rev. B **88**, 020406 (2013).
102. J. H. Mentink *et al.*, Phys. Rev. Lett. **108**, 057202 (2012).
103. I. Petrila, F. Tudorache, and S. Tascu, Phys. Lett. A **377**, 1495 (2013).
104. R. Chimata *et al.*, Phys. Rev. B **92**, 094411 (2015).
105. A. Baral and H. C. Schneider, Phys. Rev. B **91**, 100402(R) (2015).
106. G. P. Zhang, Y. Bai, and T. F. George, Phys. Rev. B **80**, 214415 (2009).
107. Z. Q. Qiu and S. D. Bader, in *Nonlinear Optics in Metals*, edited by K. H. Bennemann (Oxford Science Publications, 1998), p. 1.
108. G. P. Zhang, Y. Bai, W. Hübner, G. Lefkidis, and T. F. George, J. Appl. Phys. **103**, 07B113 (2008).
109. M. S. Si and G. P. Zhang, J. Phys.: Condens. Mat. **22**, 076005 (2010).
110. G. P. Zhang, J. Phys.: Condens. Mat. **23**, 206005 (2011).
111. G. P. Zhang, M. Q. Gu, and X. S. Wu, J. Phys.: Condens. Mat. **26**, 376001 (2014).
112. G. P. Zhang, M. S. Si, Y. H. Bai, and T. F. George, J. Phys.: Condens. Mat. **27**, 206003 (2015).
113. G. P. Zhang, Y. H. Bai, and T. F. George, Europhysics Letters **112**, 27001 (2015).
114. P. M. Haney and M. D. Stiles, Phys. Rev. Lett. **105**, 126602 (2010).
115. D. C. Ralph and M. D. Stiles, J. Magn. Magn. Mater. **320**, 1190 (2008).
116. L. He, J.- Y. Chen, J.-P. Wang and M. Li, Appl. Phys. Lett. **107**, 102402 (2015).
117. X. Li, C. T. Ma, J. Lu, A. Devaraj, S. R. Spurgeon, R. B. Comes, and S. J. Poon, Appl. Phys. Lett. **108**, 012401 (2016).
118. Y. K. Takahashi, R. Medapalli, S. Kasai, J. Wang, K. Ishioka, S. H. Wee, O. Hellwig, K. Kono and E. E. Fullerton, arXiv:1604.03488 (2016).
119. P. Wadley *et al.*, Science **351**, 587 (2016).
120. T. Satoh, R. Lida, T. Higuchi, M. Fiebig and R. Shimura, Nature Photonics **9**, 25 (2015).
121. R. Gomez-Abal, O. Ney, K. Satitkovitchai, and W. Hübner, Phys. Rev. Lett. **92**, 227402 (2004).
122. N. Ogawa, S. Seki and Y. Tokura, Scientific Reports **5**, 9552 (2015).
123. C. S. Goncalves, A. S. Silva, D. Navas, M. Miranda, F. Silva, H. Crespo and D. S. Schmool, Scientific Reports **6**, 22872 (2016).